Published in final edited form as:
Int J Mass Spectrom. 2009 October 15; 287(1-3): 8–15. doi:10.1016/j.ijms.2008.11.002.

Radical Cation/Radical Reactions: A Fourier Transform Ion Cyclotron Resonance Study of Allyl Radical Reacting with Aromatic Radical Cations

Amber L. Russell, **Henry W. Rohrs**, **David Read**, **Daryl E. Giblin**, **Peter P. Gaspar**, and **Michael L. Gross**

Abstract

A method for the study of reactions of open-shell neutrals (radicals) and radical cations is described. Pyrolysis (25–1500 °C) of thermally labile compounds, such as, 1,5-hexadiene via a Chen nozzle yields a seeded beam of reactive species in helium. The pyrolysis products are then analyzed by electron ionization (EI) or reacted with stored ions. Electron ionization of the pyrolysis products of 1,5-hexadiene shows that both the allyl radical and allene are generated. Reactions of benzene radical cations and the pyrolysis products of 1,5-hexadiene result in carbon-carbon bond formation. Those reactions of allyl radical with the benzene radical cation yield the $C_7H_7^+$ ion of *m/z* 91, permitting an unusual entry into arenium ions. The reaction of allene with benzene radical cation in contrast yields $C_9H_{10}^+$. and $C_9H_9^+$.

1. Introduction

Free radicals are important chemical intermediates [1–3] and are linked to biological damage in spongiform encephalopathies, Alzheimer's disease, heart disease, and carcinogenesis [1,4,5]. Although many elegant approaches are available to generate and study radicals, thermal decomposition coupled with MS is time-honored [6–9]. The coupling of a pyrolysis nozzle [10] with Fourier transform mass spectrometry (FTICR or FTMS) affords a new opportunity to study the reactions of radicals and radical ions.

The ability to study reactions of gas-phase ions with radicals and other reactive species has applications in basic ion chemistry and extensions into free-radical damage to biomolecules. Furthermore, there may be opportunities for conducting the reactions in solution by using, for example, electrochemical oxidation and/or lasers to generate the reactive species. These prospects provide one motivation for our development [11]. Early mass spectrometric approaches to studying radicals employed low-energy electrons, taking advantage of the ability to ionize preferentially $R^{\bullet}$, given its relatively low ionization energy relative to the appearance energy of R^+ formed as a fragment from a stable neutral molecule [12]. More recently, reports show the use of mass spectrometry (MS) for the study of gas-phase radicals and their reactions. Most are studies of stable atomic radicals reacting with ions. There is, however, a growing body of results on the reactions of polyatomic radicals with ions and neutrals. Approaches to studying polyatomic radical chemistry vary from the use of free radicals directly to that of distonic ions, in which the charge and the radical sites are

separated [13,14]. The latter species allow for the study of a radical by mass spectrometry, taking advantage of the presence of the charge site. Other approaches react ions with free radicals generated by flash photolysis [15,16], corona discharges [17], or flash pyrolysis [18]. Hydroxyl radicals generated in a corona discharge can react with electrosprayed ions to study the structure of proteins [17]. Ions are often mass-selected to react with radicals generated by flash photolysis [15.16], or pyrolysis [18]. The only example of the direct study of ion-radical reactions is that reported by Kato, et al. [18] and involved the use of a hyperthermal nozzle to generate and introduce radicals into a FA-SIFT (flowing afterglow selected ion flow tube).

Here we report an approach whereby gas-phase free radicals are prepared by pyrolysis of suitable precursors (compounds possessing a weak bond) and seeded in a supersonic beam of inert carrier gas (He) [10,19]. This radical source coupled with an FT mass spectrometer affords a means for forming and detecting free radicals and examining their reactions with gas-phase ions. The most notable advantages of this pairing are the high sensitivity and the experimental versatility of ICR [20–25].

We are pleased to contribute this paper on ion chemistry to the special issue for Charles L. Wilkins. Professor Wilkins and the senior author began working together in 1969, and together we published a number of papers in ion chemistry and on the development of analytical FT ICR MS. Appropriately, our first joint paper had also ion chemistry as its subject [26].

2. Experimental Section

2.1. Instrumentation

The FT-ICR mass spectrometer was custom-built for analytical method development [27] and consisted of a 1.2-tesla Varian electromagnet, a 4.76-cm cell, and either a Nicolet 2000 (Madison, WI) or a MIDAS (Modular ICR Data Acquisition System, National High Magnetic Field Lab, Florida State University) data system. The MIDAS system consisted of a FT-ICR cell controller, an electron-gun controller, and a PC running MIDAS software, version 3.18. The FT-ICR cell controller contained 8 DACS and 16 TTL switches and was built in the Florida State University electronic shop.

The cell detector plates were 67% transmitting stainless steel mesh. The vacuum system consisted of a custom chamber pumped by a Balzers 500 L/s turbo molecular pump backed by a two-stage roughing pump. The chamber was equipped with a Series 9 pulsed valve (General Valve, now Parker Pneutronics and General Valve/T Squared, Cleveland, OH), used for introduction of benzene, and a gas-inlet system. The pyrolysis nozzle, employed a 1 mm I.D., 0.5 mm wall thickness SiC tube (Hexoloy SA, Niagara Falls, NY). The SiC and the Al_2O_3 tubes were nested and cemented with ceramic adhesive (903HP, Cotronics, Brooklyn, NY) into the mini-Conflat flange. Electrical contact was provided by graphite disks (AXF-FQ Poco Graphite, Decatur, TX) and 0.127-mm tantalum-foil clips (Alfa Aesar, Ward Hill, MA). The tube can be heated resistively to ~ 1850 K. The temperature of the nozzle was measured by a three-color optical pyrometer focused through a window onto the exit end of the pyrolysis nozzle.

All chemicals were purchased from Sigma-Aldrich (St. Louis, Mo) and degassed before use. Typical concentrations of the radical precursor (1,5-hexadiene) were 80–300 ppm in helium with a final backing pressure of ~900 torr. Concentrations of 80–150 ppm 1,5-hexadiene were also used for experiments in which the pulsed gas was directly electron ionized, whereas higher concentrations were necessary for the studies of reactions of stored ions and products of the pyrolysis of 1,5-hexadiene.

2.2. Theoretical Calculations

Proposed reaction mechanisms with consequent structures of intermediates and the heats of formation/reaction were evaluated and calculated by molecular modeling of the precursor ions, proposed intermediates, and products. The initial survey calculations were performed by using the PM3 [28,29] semi-empirical algorithm (Spartan '02 for Linux, Wavefunction, Inc.). Further survey and second-stage calculations employed density functional theory (DFT), which requires less computational overhead than formal ab initio methods and yet incorporates dynamic correlation, has little spin contamination [30–33] and usually performs adequately giving proper geometries, energies, and frequencies. DFT is part of the Gaussian suites of programs, v98 [34] or v03 [35] (Gaussian, Inc.).

Minima and transition states were optimized to DFT level, B3LYP/6-31G(d,p), confirmed by vibrational frequency analysis. Connections of transition states were confirmed by path calculations or by projection of the normal variable associated with the imaginary frequency. Single-point energy calculations were performed at level B3LYP/6-311+G(2d,p)//B3LYP/6-31G(d,p) to which scaled zero-point and thermal-energy corrections for standard temperature and pressure were applied [36]. Minima and transition states on core mechanistically relevant pathways were then calculated by the Gaussian-3 method, G3B3 [37] using the B3LYP/6-31G(d,p) geometries. The calculated energies are reported as relative enthalpies in kcal/mol against the initial condensation adduct. It must be noted that these calculations yield information about the potential-energy surface, but ultimately fragmentation patterns are determined by kinetic processes.

3. Results and Discussion

3.1. Generation of radicals

Certain thermally labile compounds make suitable precursors for the generation of radicals. Common examples include diacyl peroxides and azo compounds. The compound, 1,5-hexadiene, represents another class; it decomposes into two identical allyl radicals at sufficiently high temperatures, making it a good precursor for the reactant.

The products of electron ionization (EI) of 1,5-hexadiene introduced through the pyrolysis nozzle (Scheme 1) included the allyl radical, as monitored by recording mass spectra as a function of nozzle temperature (Figure 1). Given that the molecular ion of 1,5-hexadiene was too low in abundance to monitor the neutral compound, we chose instead the *m/z* 67 ion formed by methyl loss. Experiments carried out at room temperature (no pyrolysis) show the formation of an ion of *m/z* 67, which was formed directly from the 1,5-hexadiene by low-energy EI (15–22 eV). As the temperature of the pyrolysis chamber was increased, the relative amounts of *m/z* 39, 40 and 41 ions increased. We attribute the *m/z* 41 ion to be ionized allyl radical, signaling its production in the pyrolysis. The *m/z* 40 ion is either a fragment of the *m/z* 41 ion or, more likely, ionized allene, formed in the pyrolysis, or both. The *m/z* 39 ion is a fragment (probably cyclopropenyl) from either the *m/z* 41 ion (loss of H_2) or ionized allene. Ionization by low-energy electrons (15 or 22 eV) was followed by standard detection by FTMS.

At a temperature of > 800 °C, allyl radical production began, as seen by the rise in the signal of *m/z* 41 ion. At higher temperatures (>850 °C), ions of *m/z* 40 appeared, suggesting a second process to make neutral allene or its isomer. Heating the nozzle resulted in a loss of ~90% of the absolute signal relative to when the nozzle is not heated. This change is attributed to a decrease in the time the valve is open and a change in flow dynamics when the nozzle is hot.

Closed-shell R^+ ions can be formed by both dissociative ionization of the unreacted precursor in the neutral beam and ionization of the free radical. Low-energy electron ionization avoided, or at least reduced significantly, the former process, although fragmentation channels can remain open at low ionizing energy if the appearance energies are sufficiently low. For example, both ions of *m/z* 82 ion [IE(1,5-hexadience) = 9.29 eV] and its fragment ion of *m/z* 67 (AE = 9.35 eV) [38] are produced at low energy, either 15 or 22 eV (set as the voltage on the filament).

The difference in ionization energies between allyl radical and allene is 1.5 eV allowing for the possible discrimination against allene at low ionization energies. Figure 1 shows the result of varying the ionization energy from 22 to 15 eV (although we could use lower ionization energies, the signal-to-noise ratios were sufficiently low to compromise solid conclusions. It should be noted that ions of *m/z* 39 can be formed from the ionization of both allyl radical and allene, the AE of ions of *m/z* 39 from allyl radical is 9.45 eV whereas that from allene is 11.47 eV [38]. In addition, pyrolysis of 1,5-hexadiene requires 58.5 kcal/mol whereas pyrolysis to allene + H_2 requires 13.8 kcal/mol additional energy [38]. Thus, differential formation of allyl radical relative to formation of allene should be favored by temperatures nearer the threshold for pyrolysis (~800 °C) as observed (Figure 1). In addition, the production of *m/z* 39 tracks more closely the production of *m/z* 41 rather than *m/z* 40 which suggests that it is derived from *m/z* 41 by H_2 elimination.

In an attempt to eliminate the presence of the ion of *m/z* 40 (presumably from the production of allene in the pyrolysis), two other allyl radical precursors were tried, allyl iodide and allyl bromide. Ions of *m/z* 40, however, were observed from both precursors. Allyl iodide was shown to be a “clean” source of allyl radical with ~90% yield in similar experiments [18]. We observed with our setup, however, significant formation of ions of *m/z* 40 upon ionization of the pyrolysis products of allyl iodide.

3.2. Reactions of radicals and radical cations

To test the feasibility of carrying out reactions of stored ions and the radicals formed by pyrolysis, we chose the reaction of benzene radical cation with allyl radical. (Scheme 2). To reduce ambiguities associated with potential reactions with neutral benzene, we carried out a dual-pulse experiment. In the first pulse, benzene vapor was introduced and ionized by a pulsed electron beam. The molecular radical cation of *m/z* 78 was isolated and stored in the ICR trap. A time delay allowed neutral benzene to be pumped away from the ICR trap before introduction of the beam of allyl radicals. This delay reduces significantly the possibility of any reactions between the neutral benzene (or any other neutral precursor of a reagent ion) and any ionized species that are produced by charge exchange. We then pulsed the 1,5-hexadiene mixture through the pyrolysis nozzle and into the trap and allowed the products to react with the stored benzene radical cations. Note that the electron beam was off at this time, so there was no electron-ionization of the allyl radical or allene if present. A delay of 10 s followed the radical pulse so that the helium could be pumped away and any ion-radical reactions could occur. Mass analysis of products followed the reaction delay. For the reaction of allyl cation with benzene, the order or introduction in the dual-pulse experiment was inverted

Scheme 2 shows possible reactions of the benzene radical cation with either the allyl radical or allene, as well as the reaction of allyl cation with neutral benzene. The dual-pulse experiment was designed to eliminate ambiguities arising from this third possible reaction (Scheme 2C).

The results (Figure 2A) of the reaction of benzene radical cation with 1,5-hexadiene when no heating was applied to the nozzle show that the stored benzene radical cation underwent

charge exchange (charge transfer) with the neutral 1,5-hexadiene resulting in *m/z* 82 and 67 ions. Heating the nozzle to a temperature of 1000 °C led to the formation of ions of *m/z* 91, 117, and 118 (Figure 2B).

To study the reaction of the allyl cation and neutral benzene (Figure 2C), we generated the allyl cation by EI of allyl bromide. Ions of *m/z* 39, 79, 81 and 131 originate from allyl bromide and can be observed in the absence of benzene. Not only was a stable ion of *m/z* 119 produced but also ions of *m/z* 91, 115 and 117 when neutral benzene was present.

Comparison of the spectra in Figures 2B and 2C shows two ions were formed: those of *m/z* 91 and 117 for the reaction of benzene radical cation with allyl radical and the reaction of allyl cation with neutral benzene. The simple adduct of the benzene radical cation and allyl radical would be an ion of *m/z* 119 ($C_9H_{11}^+$); however, under our experimental conditions, this adduct is not seen and must not be stable. The formation of the *m/z* 91 ion is explained for both reactions by a loss of C_2H_4 from the initially formed adducts. The *m/z* 118 ion was not produced in the reaction of the allyl cation and neutral benzene. It is also an unlikely product in the reaction of the allyl radical and the benzene radical cation, most likely formed via an arenium ion; its production needs further investigation.

The results of the reaction of d_6-benzene radical cation with 1,5-hexadiene (Figure 2D) are ions of *m/z* 124, 123, 122 and 96. Comparison of the spectra in Figures 2B and 2D show that the *m/z* 118 ion shifted to *m/z* 124, a shift of 6 u, owing to the six deuteria on the benzene ring. The ion of *m/z* 91, however, shifted only by 5 mass units. The initial adduct formed in the allyl radical/d_6-benzene radical cation reaction would be an ion of *m/z* 125, indicating that the ethylene expelled to form an ion of *m/z* 96 contained one of the deuteria of the benzene radical cation.

3.3. DFT calculations and mechanism

Scheme 3 shows a proposed mechanism for the loss of ethylene from the reactions of allyl radical with benzene radical cation and allyl cation with neutral benzene as based on DFT calculations. The proposed mechanism is consistent with the results from d_6-benzene labeling. The enthalpies of formation of benzene radical cation and allyl radical are calculated to be 26.8 kcal/mol greater than for formation of benzene and allyl cation, which compares favorably with 26.4 kcal/mol from empirical reference data [38]. Likewise the enthalpies of formation of benzyl cation and ethylene are calculated to be18.3 kcal/mol less than that of benzene and allyl cation, a figure identical to reference data [38]. Both set of reactants possess sufficient energy in their enthalpies of formation to drive the reaction to afford loss of ethylene.

The *m/z* 119 adduct from the reaction of an allyl radical and the benzene radical cation gains access to the energy surface in a novel and different, more highly energetic way than via the traditional reaction of a carbocation with a neutral aromatic molecule to give a Wheland intermediate [39,40].

Common losses from conventionally prepared $C_9H_{11}^+$ species are of H_2, CH_4, C_2H_4, C_3H_4 and C_6H_6 with the ethylene loss dominating; it accounts for 90–95% of the metastable-ion fragmentation from monosubsituted benzene $C_9H_{11}^+$ ions. Once the hydrogen (deuterium) shifts from the benzene ring to the side chain, all of the side-chain hydrogen atoms become ultimately equivalent in the eliminated ethylene. Classic mass spectrometric studies by Uccella and Williams [41] showed that all of the possible monosubstituted benzene structures for $C_9H_{11}^+$ can and do interconvert at rates faster than decomposition when the ions have sufficient internal energy to fragment. Both carbon-13 and deuterium labeling of the side chain show equivalence of the side chain hydrogen and carbon atoms. As shown in

Figure 2C, we observe loss of H_2, 2x H_2 and C_2H_4 from the $C_9H_{11}^+$ species formed in the reaction of benzene and allyl cation; however, for the more energetic preparation of $C_9H_{11}^+$ by the reaction of the benzene radical cation and allyl radical, only loss of C_2H_4 occurs (Figure 2B). (The *m/z* 118 and 117 ions were later shown to have another origin). Note that the pathway for the $C_9H_{11}^+$ species to lose ethylene, as represented in Scheme 3, involves only a facile proton transfer via transition state TS_{2-3} and two facile hydride transfers via transition states TS_{1-2} and $TS_{3\text{-}I}$, leading to spontaneous, homolytic CC bond cleavage and ethylene loss. Such a series of steps can by significantly promoted by additional internal energy of the initial $C_9H_{11}^+$ precursor. (For further details of the immediate potential surface, see the Scheme in the Supplementary Data).

We monitored the products of the reaction of allyl radical and benzene radical cation by recording mass spectra as a function of nozzle temperature (Figure 3). Experiments carried out at room temperature showed the formation of ions of *m/z* 67 and 82. Heating the nozzle to a temperature of 800 °C afforded an ion of *m/z* 91; additional heating gave rise to the ions of *m/z* 117 and 118. The formation of an ion of *m/z* 91 tracks well with that of the *m/z* 41 ion (Figure 1), whereas the formation of *m/z* 117 and 118 ions tracks with that of the *m/z* 40 ion, suggesting the ions at *m/z* 117 and 118 have their origin with allene rather than directly with allyl radical.

We then carried out the reaction of neutral allene with the benzene radical cation (Figure 4); this reaction gives ions of *m/z* 117 and 118 but not one of *m/z* 91.

3.4. Reactions of radicals with other aromatic radical cations

We expanded these studies to include the reactions of other radical cations with allyl radical; both thiophene and furan radical cations reacted, whereas pyridine and toluene radical cations did not. The reactions of thiophene and furan radical cations led to an $[M + 13]^+$ product formed by the loss of ethylene from the initially formed adduct, analogous to the *m/z* 91 ion formed in the reaction with the benzene radical cation. The spectrum in Figure 5A shows the result of 1,5-hexadiene reacting with the stored furan radical cation. Heating the nozzle to a temperature above 800 °C showed an increase in the amount of protonated furan (*m/z* 69), and the reaction product $[M + 13]^+$ (*m/z* 81) (Figure 5B).

Hydrogen radical transfer did not occur in the reaction of benzene radical cation and allyl radical; however, it was the dominate product in the reaction of furan radical cation. The reaction with the thiophene radical cation also shows only the formation of $[M + 13]^+$ (*m/z* 97) (Figure 6B) arising by loss of ethylene from the initial complex. These reactions are novel, providing more evidence for the reaction of radicals with radical cations. Expanding the scope of these reactions to include closed-shell ions of biomolecules would also be of interest and relevance in biology.

3.5. Experimental timing for the radical-radical cation reaction

It is of importance to establish whether the reactions occurring in this system happen on the first pass of radicals through the FT ICR trap, or if the radicals pass through the trap, collide with the walls and/or with other neutrals, before diffusing into the trap and reacting. The latter could present an opportunity for the radicals to rearrange or fragment. To test, we monitored the reactions of benzene radical cation with the pyrolysis products of 1,5-hexadiene while temporally ejecting the benzene radical cation from the trap, effectively quenching the reaction as a function of time (Figure 7). If the reactant ions are ejected prior to the super sonic beam pulse, no reaction can occur. If the neutral radicals react on the first pass, then the maximum product abundance will occur promptly. If, however, the reactions have a time offset, this would indicate that the radicals react after passing through the trap,

colliding with vacuum-chamber walls and other neutrals, and then diffuse back into the ICR trap.

Figure 8 shows the result of this “double resonance” experiment for the reaction of the benzene radical cation and the 1,5-hexadiene pyrolysis products. The ions of *m/z* 67 and 91 were seen at the beginning of the pulse, whereas the ions of *m/z* 117 and 118 were shifted to a later time. These results indicate that the ions of *m/z* 67 and 91 were generated during the first pass of the radical beam through the trap, whereas the other products, particularly the *m/z* 117 and 118 ions, were formed after the radicals had collided with other molecules or the vacuum-chamber walls. It is also possible that allene was formed from allyl in these collisions.

4. Conclusion

The reactions of radicals and radical ions can be conducted by the approach of Kato, et al. [18] and the one we introduce here, and they are uncomplicated by the effects of charge on the reactivity of the radical. The use of an FT ICR instrument makes the method widely available to many laboratories in which ion chemistry is investigated.

Although the velocities of the stored ions and the radical beam are mismatched, the reaction still occurred, indicating that the translational energy of the allyl radicals was thermally damped, consistent with the results of the double resonance experiment. Correcting this mismatch in energy may be accomplished by increasing the translational energy of the stored ions by either exciting their cyclotron motion or by SORI, affording “softer” collisions between the ions and radicals and better reaction yields.

Supplementary Material

Refer to Web version on PubMed Central for supplementary material.

Acknowledgments

Thanks to Professors. K. Kelton (Wash. U.) and G. B. Ellison (U. Col.) for equipment, R. A. Loomis (Wash. U.) and P. Chen (ETH) for advice on beam experiments, and Poco Graphite for donating graphite. Funding was provided by NIH (P41RR000954), NSF CHE-9981715 and GAANN (P200A80221). This work made use of the Washington University Computational Chemistry Facility, supported by NSF grant CHE-0443501

References

1. Schoneich C, Nauser TJ. J Am Chem Soc 2003;125:2042. [PubMed: 12590520]
2. Wardman, P. Biothiols in Health and Disease. Packer, L.; Cadenas, E., editors. Marcel Dekker; New York: 1995. p. 1
3. Stubbe J, van der Denk WA. Chem Rev 1998;98:705. [PubMed: 11848913]
4. Dizdaroglu M, Gajewski E, Reddy P, Margolis SA. Biochem 1989;28:3625. [PubMed: 2545260]
5. Balasubramanian D, Kanwar R. Mol Cell Bio 2002;234/235:27.
6. Belchetz L, Rideal EK. J Am Chem Soc 1935;57:1168.
7. Eltenton GC. J Chem Phys 1942;10:403.
8. Eltenton GC. J Chem Phys 1947;15:455.
9. Harrison, AG. Mass Spectrometry of Organic Radicals. In: McLafferty, FW., editor. Mass Spectrometry of Organic Ions. Academic Press Inc; New York: 1963. p. 207
10. Kohn DW, Clauberg H, Chen P. Rev Sci Instrum 1992;63:4003.
11. Valko M, Leibfritz D, Moncol J, Cronin MTD, Mazur M, Telser J. Int J Biochem Cell Biol 2007;39:44. [PubMed: 16978905]
12. Lossing FP, Tickner AW. J Chem Phys 1952;20:907.

13. Stirk KM, Kiminkinen LK, Kenttamaa HI. Chem Rev 1992;7:1649.
14. Yu SJ, Holliman CL, Rempel DL, Gross ML. J Am Chem Soc 1993;115:9676.
15. LeBras, G. Reactions of NO_3 Radicals in the Gas Phase. In: Alfassi, ZB., editor. N-Centered Radicals. Wiley; Chichester, UK: 1998. p. 259
16. Griffiths IW. Advances in Mass Spectrometry 1998;14:B013670/1–B013670/13.
17. Maleknia SD, Chance MR, Downard KM. Rapid Commun Mass Spec 1999;13:2352.
18. Zhang X, Bierbaum VM, Ellison GB, Kato SJ. Chem Phys 2004;120:3531.
19. Blush JA, Clauberg H, Kohn DW, Minsek DW, Zhang X, Chen P. Acc Chem Res 1992;25:385.
20. Zubarev RA, Horn DM, Fridriksson EK, Kelleher NL, Kruger NA, Lewis MA, Carpenter BK, McLafferty FW. Anal Chem 2000;72:563. [PubMed: 10695143]
21. Nielsen ML, Budnik BA, Haselmann KF, Olsen JV, Zubarev RA. Chem Phys Let 2000;330:558.
22. Cody RB, Freiser BS. Anal Chem 1979;51:547.
23. McLafferty FW, Amster IJ. Int J Mass Spectrom Ion Proc 1986;72:85.
24. Aaserud DJ, Guan ZA, Little DP, McLafferty FW. J Mass Spectrom Ion Proc 1997;167–168:705.
25. Marshall AG. Int J Mass Spectrom Ion Proc 2000;200:331.
26. Gross ML, Wilkins CL. Tetrahedron Lett 1969;44:3875.
27. Ledford EB Jr, White RL, Ghaderi S, Wilkins CL, Gross ML. Anal Chem 1980;52:2450.
28. Stewart JJP, Frank JS. J Comp Chem 1989;10:209.
29. Stewart JJP, Frank JS. J Comp Chem 1989;10:221.
30. Wittbrodt JM, Schlegel HB. Chem Phys 1996;105:6574.
31. Baker J, Scheiner A, Andzelm J. J Chem Phys Lett 1993;216:380.
32. Laming GJ, Hardy NC, Amos RD. Mol Phys 1993;80:1121.
33. Nicolaides A, Smith DM, Jensen F, Radom LJ. J Am Chem Soc 1997;119:8083.
34. Frisch, MJ.; Trucks, GW.; Schlegel, HB.; Scuseria, GE.; Robb, MA.; Cheeseman, JR.; Zakrzewski, VG.; Montgomery, JA., Jr; Stratmann, RE.; Burant, JC.; Dapprich, S.; Millam, JM.; Daniels, AD.; Kudin, KN.; Strain, MC.; Farkas, O.; Tomasi, J.; Barone, V.; Cossi, M.; Cammi, R.; Mennucci, B.; Pomelli, C.; Adamo, C.; Clifford, S.; Ochterski, J.; Petersson, GA.; Ayala, PY.; Cui, Q.; Morokuma, K.; Malick, DK.; Rabuck, AD.; Raghavachari, K.; Foresman, JB.; Cioslowski, J.; Ortiz, JV.; Baboul, AG.; Stefanov, BB.; Liu, G.; Liashenko, A.; Piskorz, P.; Komaromi, I.; Gomperts, R.; Martin, RL.; Fox, DJ.; Keith, T.; Al-Laham, MA.; Peng, CY.; Nanayakkara, A.; Gonzalez, C.; Challacombe, M.; Gill, PMW.; Johnson, B.; Chen, W.; Wong, MW.; Andres, JL.; Gonzalez, C.; Head-Gordon, M.; Replogle, ES.; Pople, JA. Gaussian 98, Revision A 07. Gaussian, Inc; Pittsburgh PA: 1998.
35. Frisch, MJ.; Trucks, GW.; Schlegel, HB.; Scuseria, GE.; Robb, MA.; Cheeseman, JR.; Montgomery, JA., Jr; Vreven, T.; Kudin, KN.; Burant, JC.; Millam, JM.; Iyengar, SS.; Tomasi, J.; Barone, V.; Mennucci, B.; Cossi, M.; Scalmani, G.; Rega, N.; Petersson, GA.; Nakatsuji, H.; Hada, M.; Ehara, M.; Toyota, K.; Fukuda, R.; Hasegawa, J.; Ishida, M.; Nakajima, T.; Honda, Y.; Kitao, O.; Nakai, H.; Klene, M.; Li, X.; Knox, JE.; Hratchian, HP.; Cross, JB.; Bakken, V.; Adamo, C.; Jaramillo, J.; Gomperts, R.; Stratmann, RE.; Yazyev, O.; Austin, AJ.; Cammi, R.; Pomelli, C.; Ochterski, JW.; Ayala, PY.; Morokuma, K.; Voth, GA.; Salvador, P.; Dannenberg, JJ.; Zakrzewski, VG.; Dapprich, S.; Daniels, AD.; Strain, MC.; Farkas, O.; Malick, DK.; Rabuck, AD.; Raghavachari, K.; Foresman, JB.; Ortiz, JV.; Cui, Q.; Baboul, AG.; Clifford, S.; Cioslowski, J.; Stefanov, BB.; Liu, G.; Liashenko, A.; Piskorz, P.; Komaromi, I.; Martin, RL.; Fox, DJ.; Keith, T.; Al-Laham, MA.; Peng, CY.; Nanayakkara, A.; Challacombe, M.; Gill, PMW.; Johnson, B.; Chen, W.; Wong, MW.; Gonzalez, C.; Pople, JA. Gaussian 03, Revision C 02. Gaussian, Inc; Wallingford, CT: 2004.
36. Scott AP, Radom LJ. J Phys Chem 1996;100:16502.
37. Baboul AG, Curtiss LA, Redfern PC, Raghavachari K. J Chem Phys 1999;110:7650.
38. Lias SG, Bartmess JE, Liebman JF, Holmes JL, Levine RD, Mallard WG. Gas-Phase Ion and Neutral Thermochemistry. J Phys Chem Ref Data 1988;17(Suppl No 1)
39. Miller D, Lay JO, Gross ML. J Chem Soc, Chem Commun 1982;17:970.

40. Smith, MB.; March, J. March's Advanced Organic Chemistry. John Wiley & Sons, Inc; New York: 2001.
41. Uccella NA, Williams DH. J Amer Chem Soc 1972;94:8778.

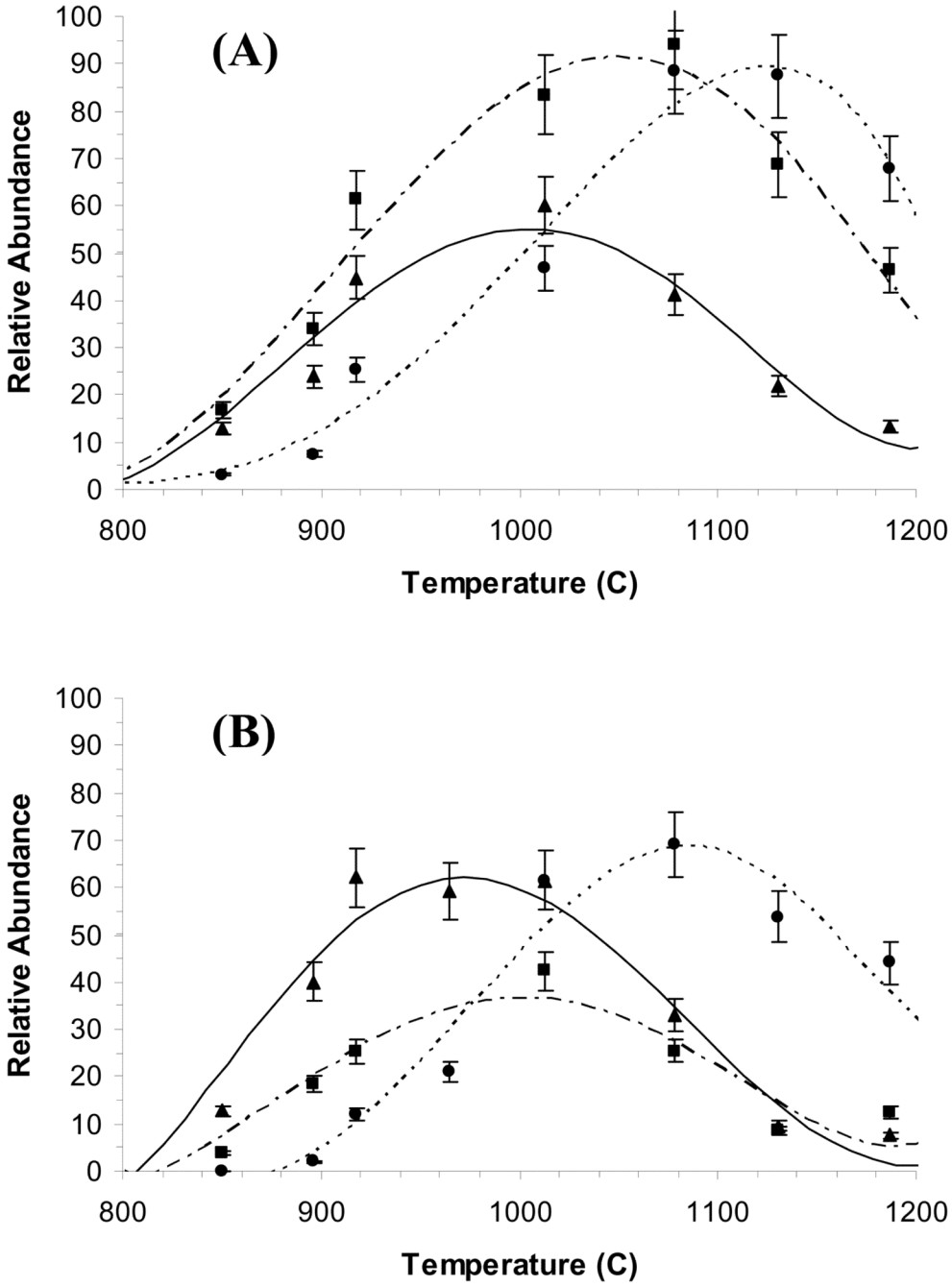

Figure 1.
Thermolysis products of 1,5-hexadiene with increasing temperature of the nozzle (A) 22 eV (B) 15 eV.
m/z 39, *m/z* 40, *m/z* 41

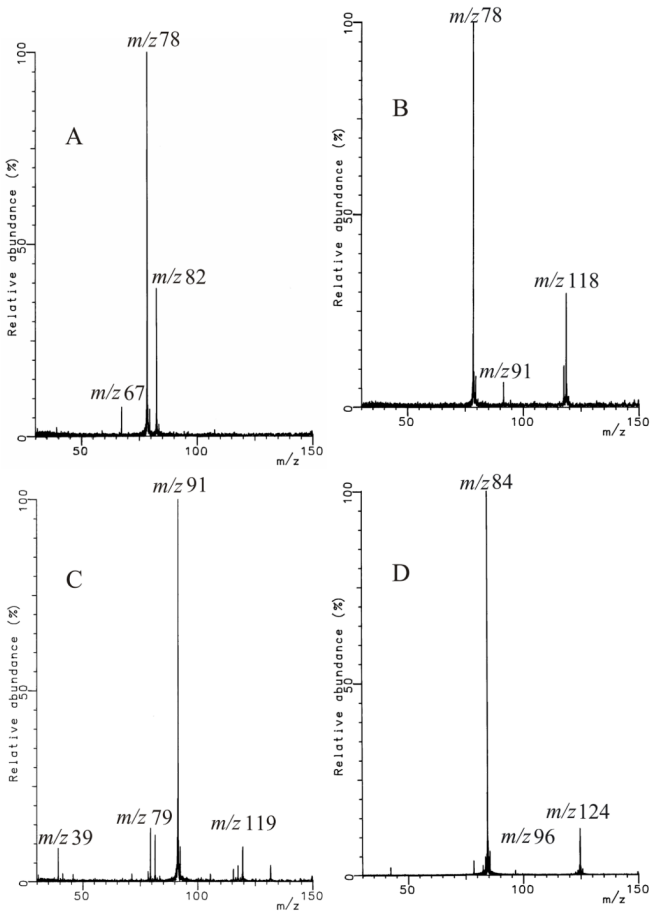

Figure 2.

Dual-pulse ion-neutral reaction between benzene radical cation and 1,5-hexadiene (A), or allyl radical (B). Reaction of allyl cation (generated from allyl-bromide) with neutral benzene (C). Reaction of d_6-benzene radical cation and allyl radical (D). Allyl radical was generated by pyrolysis of 1,5-hexadiene.

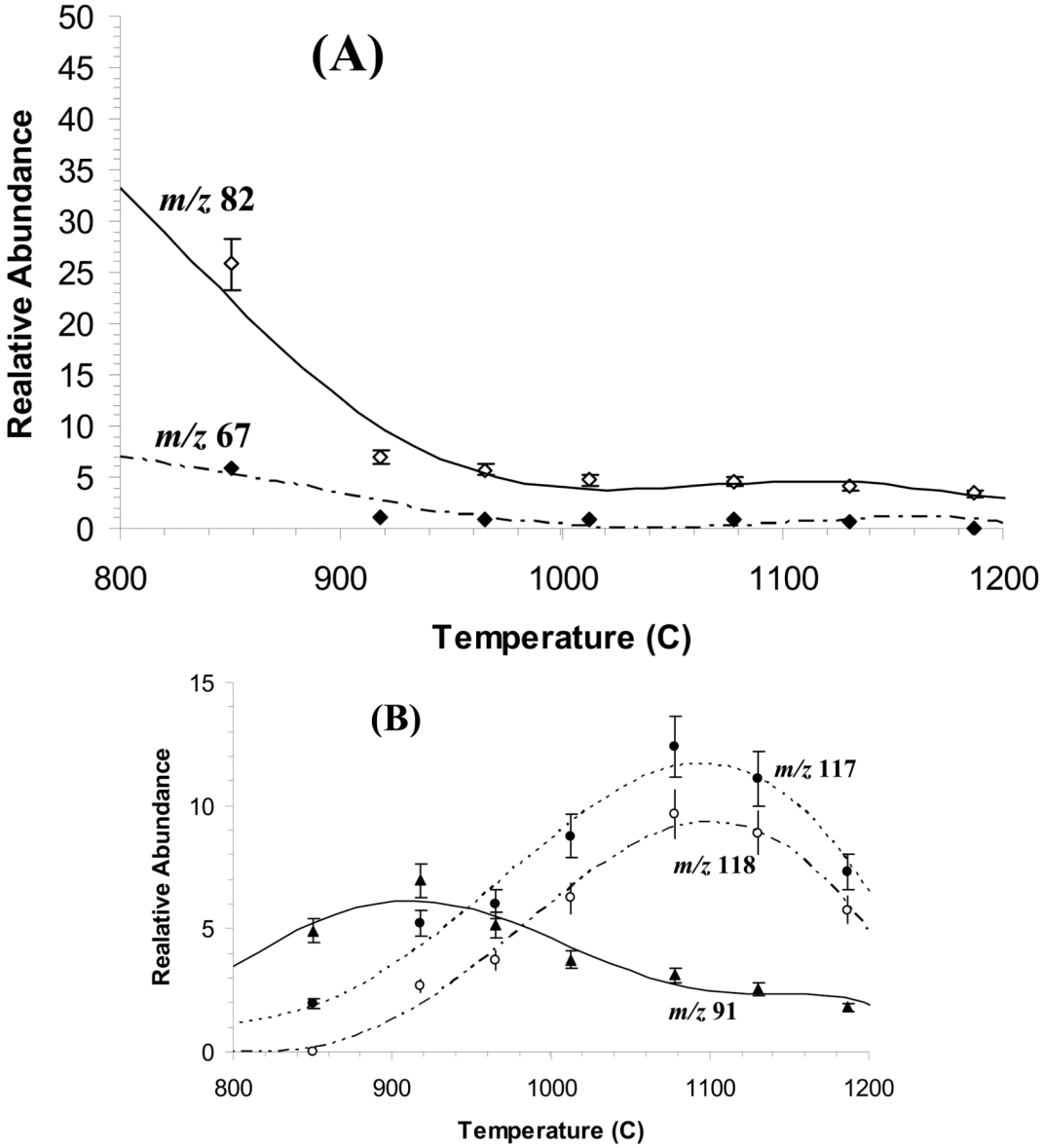

Figure 3.
Reaction of benzene radical cation with pyrolysis products of 1,5-hexadiene as a function of temperature.

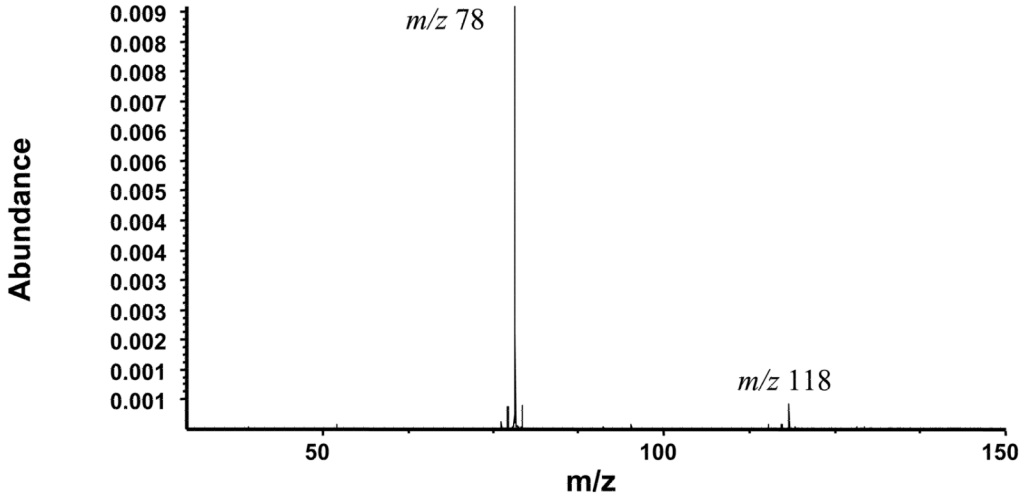

Figure 4.
Reaction of allene with the benzene radical cation gives *m/z* 118 and 117 ions.

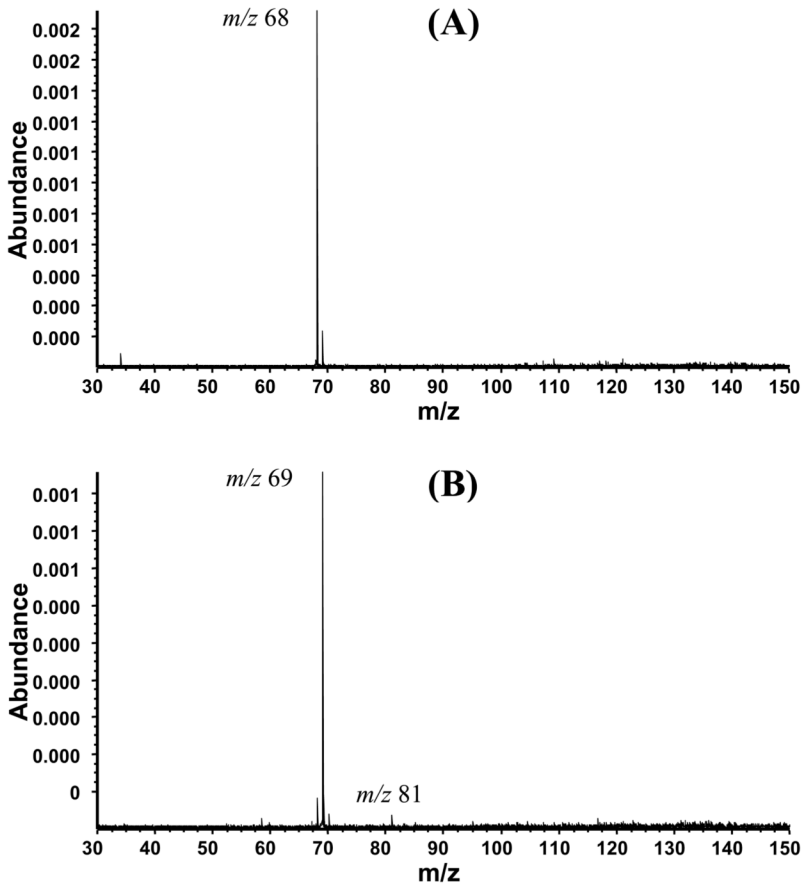

Figure 5.

Reaction of furan with 1,5-hexadiene (A) and allyl radical (B). For (A), the nozzle was pulsed but not heated. For (B) the nozzle was pulsed and heated (800 °C), producing neutral allyl radical, which reacted with thiophene radical cation to give *m/z* 81 ion.

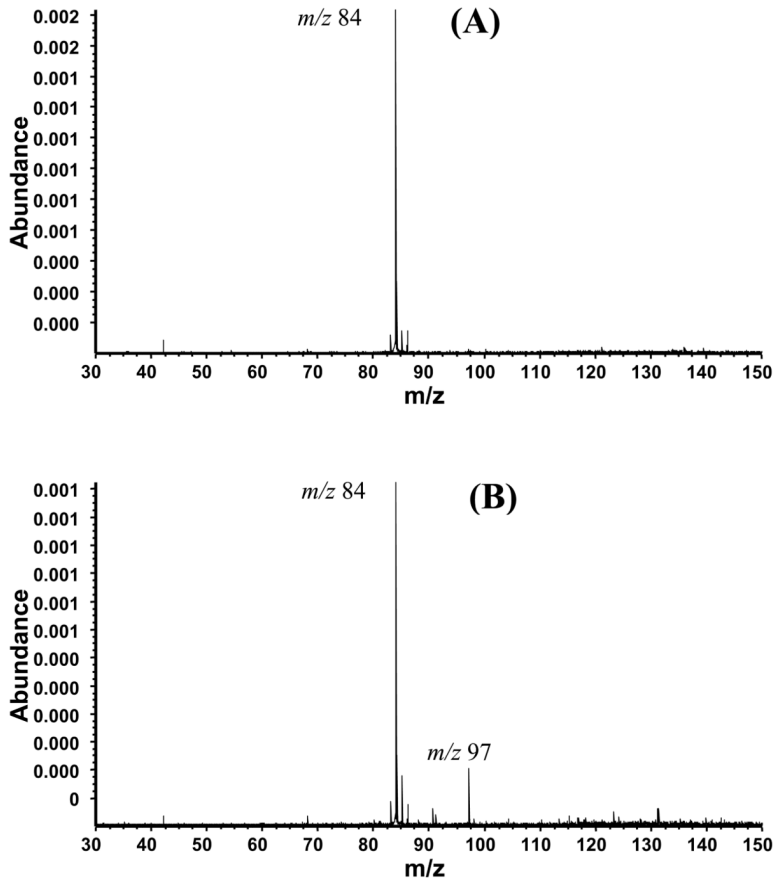

Figure 6.

Reaction of thiophene with 1,5-hexadiene (A) and allyl radical (B). (A) The nozzle was pulsed but not heated. The unreacted thiophene radical cation is of *m/z* 84. (B) The nozzle was pulsed and heated (800 °C), producing neutral allyl radical, which reacted with thiophene radical cation to give the *m/z* 97 ion.

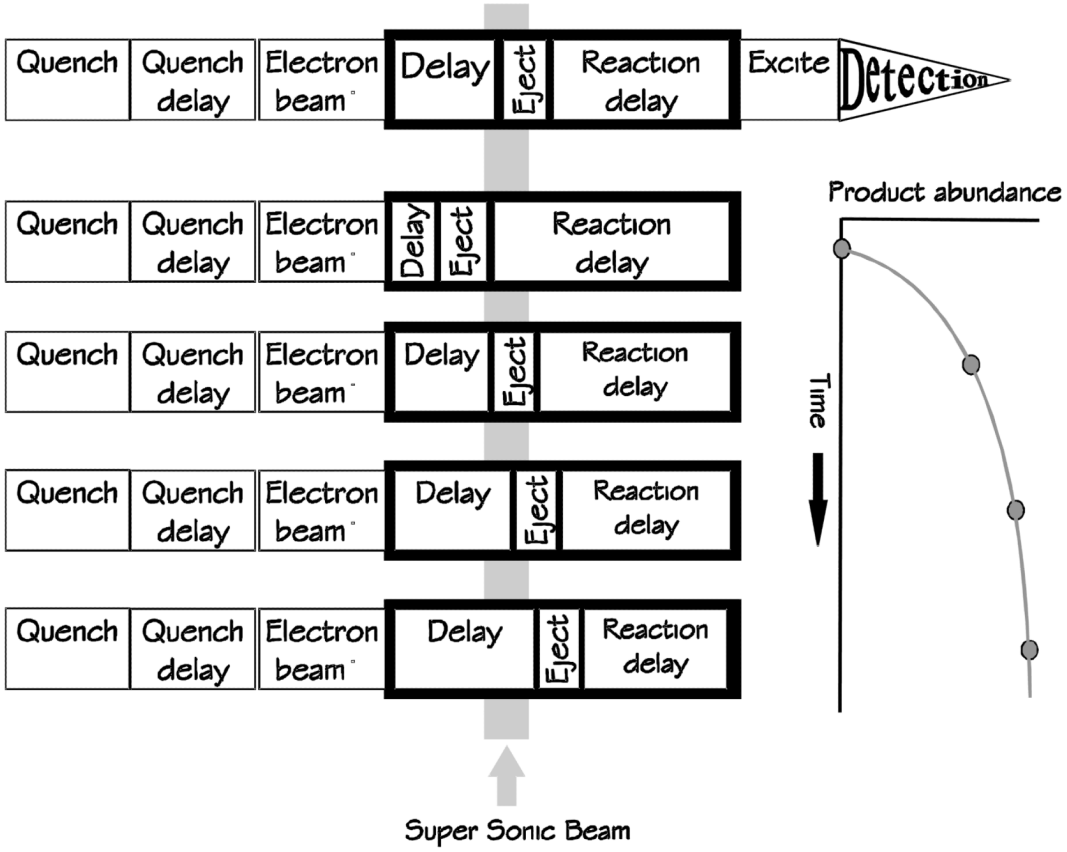

Figure 7.
Double Resonance Experiment to measure the time-dependence of product formation. The top sequence shows the experiment format. The second through fifth sequences show the ejection of reactant benzene ions at increasing times with respect to the super sonic beam.

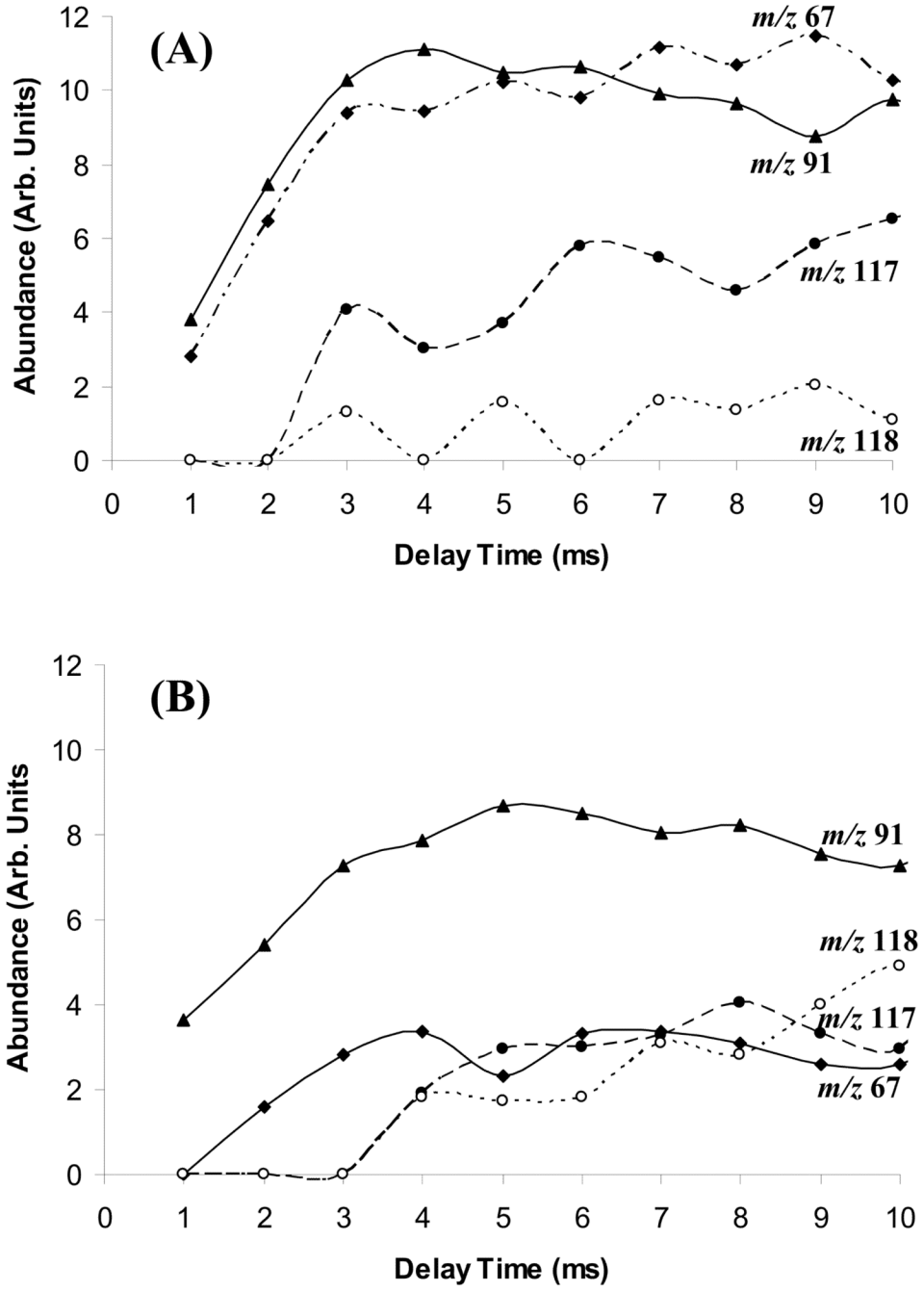

Figure 8.
Ion production as a function of delay time in a double-resonance experiment. (A) at 920 °C; (B) at 1190 °C.

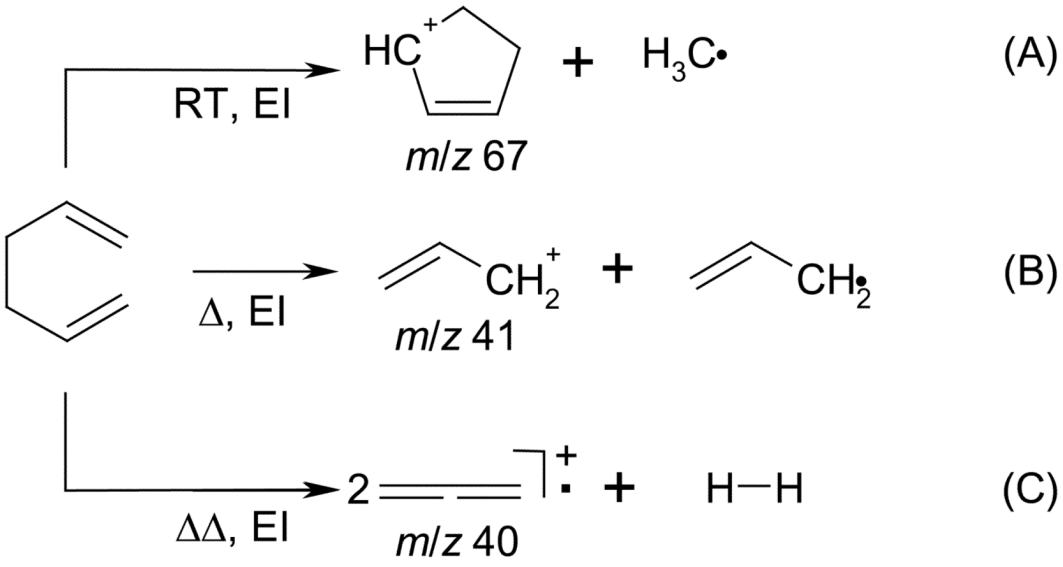

Scheme 1.
Electron ionization products of 1,5-hexadiene when pulsed through the pyrolysis nozzle at room temperature (A) and at higher temperatures (B and C).

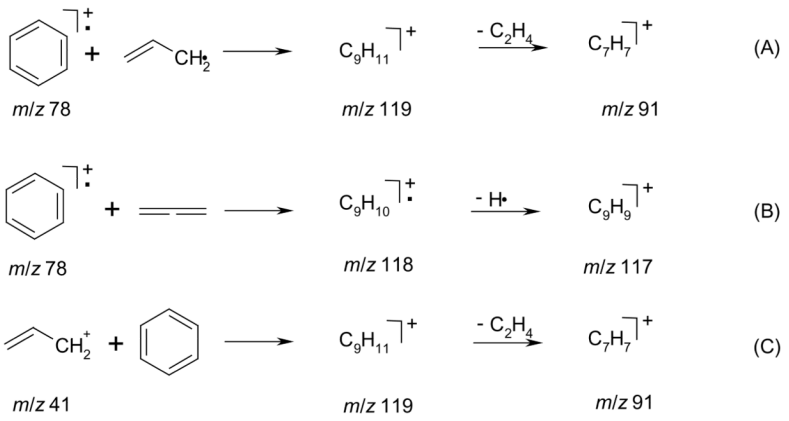

Scheme 2.
Reactions of benzene radical cation with allyl radical (A) or allene (B). Reaction of allyl cation with neutral benzene (C).

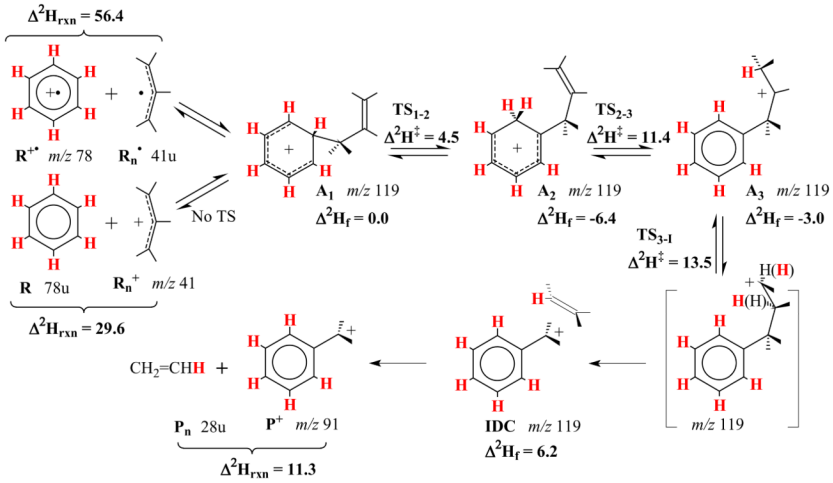

Scheme 3.

Mechanism for the loss of ethylene from $C_9H_{11}^+$ (*m/z* 119). Relative enthalpies Δ^2H_f, Δ^2H_{rxn}, $\Delta^2H^{\ddagger}$ in kcal/mol, were calculated by G3B3 theory (TS = transition state, IDC = ion-dipole complex). Sites and fates from d_6 labeling are shown in red.